Transaction A: Civil Engineering
Vol. 16, No. 3, pp. 238–248

SCIENTIA IRANICA

Uniform Hazard Response Spectra and Ground Motions for Tabriz

H. Moghaddam[1], N. Fanaie[1,*] and H. Hamzehloo[2]

Abstract. *Tabriz has experienced several large destructive historical earthquakes in the past. Due to the absence of ground motion records in this area, a simulation of future events based on a regional seismicity information and ground motion model is necessary. Based on a maximum likelihood method, earthquake magnitude is estimated for a 10% probability of exceedance within 50 years (475-year return period) and its corresponding strong ground motions have been simulated using stochastic finite fault modeling. Using different stress parameters, suites of ground motions have been simulated for a return period of 475 years and their spectral accelerations have been compared with the corresponding uniform hazard spectrum. It is observed that the fit between simulated spectra and its corresponding uniform hazard spectrum has been improved including the directivity effect especially at high periods.*

Keywords: *Seismic hazard deaggregation; Stochastic finite fault; Stress parameter; Tabriz.*

INTRODUCTION

The Probabilistic Seismic Hazard Analysis (PSHA) is generally used to display relative contributions to the hazard from different values of the random components of the problem, specifically magnitude (M), source to site distance (R) and ε, a deviation measure of the ground motion from a predicted (median) value.

PSHA provides infinite choices for the users and decision-makers. Even though PSHA involves very complicated processes, the end results (hazard curves) are simple. Hazard curves give an annual probability range of exceeding (or return period) versus a range of ground motion values. On the other hand, the process of determining the relative contribution, in terms of magnitude and distance, is called deaggregation.

To make the results of the probabilistic seismic hazard assessment more effective, a deaggregation procedure can be used for engineering purposes. Hazard can be represented by single or multiple earthquakes of certain M and R (so-called dominant earthquakes) that determine the motion in a certain frequency range. Ground motion parameters for engineering purposes can be obtained (generated or selected) for these (M, R) pairs [1]. The representation of hazard can be improved by a deaggregation over latitude and longitude rather than distance [2-4]. An examination of seismic hazard deaggregation enables investigators to determine the distance and azimuth to predominant sources and their magnitudes. Specific faults that contribute significantly to the seismic hazard can be identified at a given site [4].

Several destructive historical earthquakes that have occurred in Tabriz are shown in Figure 1. A simulation of strong ground motions for future events, based on regional seismicity information and a ground motion model, is necessary due to the absence of ground motion records in this area. In this regard, seismic hazard deaggregation and a maximum likelihood method are applied to estimate magnitude for a return period of 475 years. Then, we have applied the stochastic finite fault modeling to simulate ground motions in Tabriz at selected observation points.

TECTONIC AND SEISMICITY OF TABRIZ REGION

Tabriz is located in the Araxes structural block of the northwest of Iran; the southwest continuation of the western Alborz Mountains toward the Caucasus. The

1. *Department of Civil Engineering, Sharif University of Technology, Tehran, P.O. Box 11155/8639, Iran.*
2. *International Institute of Earthquake Engineering and Seismology, Tehran, Iran.*
*. *Corresponding author. E-mail:nader.fanaie@mehr.sharif.edu*

Received 23 September 2007; received in revised form 17 February 2008; accepted 3 March 2008

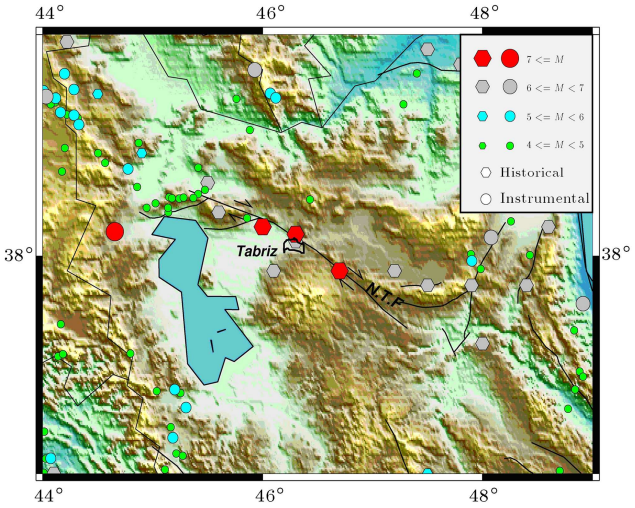

Figure 1. Historical and instrumental seismicity around Tabriz, N.T.F is North Tabriz Fault.

north Tabriz fault is a complex northwest trending structure that shows evidence of a right lateral strike slip displacement (observed on aerial photographs) and a vertical displacement with the north side up.

The north Tabriz fault, being active in the Tabriz region and having a clear surface expression, has experienced several large destructive earthquakes in the past. It has an average strike of NW-SE over a length of about 150 km and appears to be generally close to the vertical direction in the dip [5]. A right lateral movement along this fault, documented by Berberian and Arshadi [6], can also be seen clearly in the field [7]. The north Tabriz fault merges the northwest with a zone of reverse faults that turn west-southwest in the northern area of Lake Urumiyeh and southeast with another zone of reverse faults turning east-northeast [8].

Although the Tabriz fault has not generated any large earthquake during the last two centuries, many historical earthquakes have occurred in the Tabriz region (e.g. the 858, 1042, 1304, 1593, 1641, 1717, 1721, 1780 and 1786) [8]. Tabriz has been damaged several times by large earthquakes; e.g. the 1042 ($Ms = 7.6$), 1721 ($Ms = 7.7$), 1780 ($Ms = 7.7$) and 1786 ($Ms = 6.3$). The 1780 earthquake ruptured the northwest part of the north Tabriz fault, whereas the 1721 event ruptured the southeast part of the fault [5]. The earthquakes with magnitudes over 5.0 occurred in a radius of 150 km from Tabriz as shown in Table 1.

The historical seismicity of the north Tabriz fault suggests that the recurrent time intervals are about

Table 1. List of all occurred earthquakes around Tabriz.

Year	Month	Day	Latitude	Longitude	Ms	Distance (km)
858			38.100 N	46.300 E	6	6
1042	11	4	38.100 N	46.300 E	7.6	6
1304	11	7	38.500 N	45.500 E	6.7	83
1593			37.800 N	47.500 E	6.1	112
1641	2	5	37.900 N	46.100 E	6.8	23
1717	3	12	38.100 N	46.300 E	5.9	6
1721	4	26	37.900 N	46.700 E	7.7	42
1780	1	8	38.200 N	46.000 E	7.7	28
1786	10		38.300 N	45.600 E	6.3	64
1843	4	18	38.700 N	44.900 E	5.9	139
1879	3	22	37.800 N	47.900 E	6.7	147
1883	5	3	37.900 N	47.200 E	6.2	84
1900	2	24	38.450 N	44.870 E	5.4	129
1905	1	9	38.000 N	46.000 E	6.2	24
1930	5	6	38.150 N	44.650 E	7.2	141
1931	4	27	39.340 N	45.970 E	6.4	145
1934	2	22	38.230 N	45.040 E	5.7	109
1965	2	10	37.660 N	47.090 E	5	85
1968	6	9	39.071 N	46.090 E	5	114
1968	9	1	39.142 N	46.180 E	5.1	121
1981	7	23	37.141 N	45.230 E	5.6	136
1997	3	2	37.864 N	47.865 E	4.6	142

250 years, taking the whole set of earthquakes into account during 700 years and considering the strongest earthquakes [9]. Hessami et al. [5] propose a recurrence interval of 821 ± 176 years based on paleoseismological studies. They found evidence for at least four events during the past 3600 years. Masson et al. [9] suggest 8 mm/yrs of right lateral displacement for the WNW-ESE faults in the Tabriz region using GPS surveys.

The north Tabriz fault, however, has been seismically inactive during the last two centuries. Therefore, it is important to estimate ground motion parameters regarding future earthquakes, which may occur in the north of Tabriz; the most potential seismic source adjacent to Tabriz.

METHOD

Seismic Hazard Deaggregation

For a given site hazard, the annual Probability of Exceedance (PE) of a specified ground motion or spectral acceleration, u_0, is as follows:

$$\Pr[u > u_0] = \sum_M \sum_R \sum_i \text{rate (source } (M,R)) \; Wt(A_i) \Pr[u > u_0 | M, R, A_i]. \quad (1)$$

The first summation is over source magnitude, M, from $M_{\min}$ to $M_{\max}$, M being the moment magnitude. The second summation is over site to source distance, R, and finally, the third summation is over the different models of attenuation; each having a preassigned weight, $Wt(A_i)$. The rate factor in Equation 1 is the mean annual rate of source occurrence (M, R). The conditional probability factor, $\Pr[\bullet]$, is the probability of exceedance of the ground motion level, given the source magnitude (M), distance (R) and the models of seismic wave attenuation (A_i). Epistemic uncertainty in the ground motion for a certain source is usually treated using a number of attenuation models [4].

The summation of the annual frequencies in Equation 1 is generally called an aggregation of the contributions from each elementary source. Deaggregation is exactly the opposite of aggregation in which the contributions are separated versus magnitude and distance. Performing a geographic hazard deaggregation allows us to determine predominant sources of seismic hazard [4].

Following Frankel [10] and current practice in PSHA, we consider response spectral acceleration or peak ground motion acceleration, u, from specific faults or source cells. While S_k, the kth source, has a limit range of magnitude, the conditional probability of u exceeding u_0 (the reference ground motion) gives the occurrence of an earthquake in this magnitude range: S_k as $P[u > u_0 | s_k]$. We denote the annual frequency of earthquakes with the same magnitude range in S_k as f_k. From the kth source (S_k being the annual mean number of exceedances at the site), h_k can be calculated according to Harmsen et al. [3] as below:

$$h_k = f_k P[u > u_0 | S_k]. \quad (2)$$

The relative contributions of sources are often displayed in terms of a specified range of magnitude and distance. The combining process of contributions into an array of magnitude and distance ranges is called binning. Let us consider $h_i = \Sigma h_k$, where the sum is over k, such that $S_k \in \text{bin}_i$. Weigh the ith bin's contribution, and k is an index over both location and magnitude. According to Frankel et al. and Harmsen et al. [11,3] the distribution of potential seismic sources with well defined magnitudes and distances is as follows:

$$\overline{M} = \frac{\sum_i M_i h_i}{\sum_i h_i}, \qquad \overline{R} = \frac{\sum_i R_i h_i}{\sum_i h_i}, \quad (3)$$

where M_i is the $\overline{M}$ of sources in bin i and R_i is the $\overline{R}$ of sources in bin i. The sum over i includes contributions from all sources. $\overline{M}$ and $\overline{R}$ are independent of bin sizes and locations and other binning details. These parameters can be used for determining the design earthquakes [12]. Design earthquakes are needed for the time histories and duration of strong ground motion analyses [13]. Events inducing the exceedance of any given level of ground motion intensity (e.g., Sa) computed via PSHA are summarized in terms of mean values, $\overline{M}$ and $\overline{R}$ [14]. These mean values, globally evaluated for all seismic sources around the site, are used for further investigation of the sensitivity of seismic hazard calculations to the statistical uncertainties in models and parameters.

Deaggregation of a probabilistic seismic hazard is helpful in determining the location of the most probable source that may contribute to hazard. This determination (a reasonable choice for a scenario earthquake in the simulation) can be specified in the form of average distance and magnitude. This median ground motion from the earthquake that dominates the hazard is not generally equal to the probabilistic ground motion [3].

In this study, attenuation equations developed by Sadigh [15], Atkinson & Silva [16] and Campbell & Bozorgnia [17] have been considered to model epistemic uncertainty, having potential errors in the physical description of seismic wave attenuation and associated source size. These relations are selected because the developed attenuation relations in Iran cannot predict ground motions at distances below 30 km due to the lack of data. Equal weights are considered for these attenuation relationships based on which a probabilistic seismic hazard analysis has been applied.

In our study, the most predominant source is the north Tabriz fault on which several destructive earthquakes occurred. Based on paleoseismological studies, we have considered the slip rate for the north Tabriz fault [5]. Therefore, the rate at which the earthquake occurred in the PSHA analysis is mm/yr instead of the conventional activity rate (number of events/yr with $M > M_{\min}$).

Stochastic Finite Fault Modeling Approach

The stochastic model is widely used to simulate acceleration time histories. The goal of this method is to generate a transient time series having a stochastic character and a spectrum matched to the specified desired amplitude [18]. A window is applied to a time series of Gaussian noise with zero mean and unit variance. The windowed time series is transformed to the frequency domain and the amplitude spectrum of the random time series is multiplied by the desired spectrum. Transformation back to the time domain results in a stochastic time series whose amplitude spectrum is the same as the desired one on average. The application of this method clearly requires specification of the target amplitude spectrum of the earthquake to be simulated. Therefore, the stochastic method needs a model that specifies the Fourier spectrum of ground motion as a function of magnitude and distance. The acceleration spectrum is usually modeled by a spectrum with an ω^2 shape, where ω is angular frequency [18-21]. In the Brune model, the spectrum is derived from an instantaneous shear dislocation at a point. The acceleration spectrum of the shear waves, $A(f)$, at hypocentral distance R from an earthquake is calculated by:

$$A(f) = (CM_0(2\pi f)^2/[1+(f/f_0)^2])\exp(-\pi fR/Q\beta) \exp(-\pi f\kappa)D(f)/R, \quad (4)$$

where M_0 is the seismic moment and f_0 is the corner frequency which is given by:

$$f_0 = 4.9 * 10^6 \beta(\Delta\sigma/M_0)^{1/3}, \quad (5)$$

where $\Delta\sigma$ is the stress parameter in bars, M_0 is in dyne-cm and β is the shear wave velocity in km/s. The constant $C = \Re_{\theta\varphi}FV/(4\pi\rho\beta^3)$, where $\Re_{\theta\varphi}$ is the root mean square of radiation coefficients (average value of 0.55 for shear waves), F is the free surface amplification (2.0), V is partitioned into two horizontal components (0.71), ρ is density and R is hypocentral distance [18]. The term, $\exp(-\pi f\kappa)$, is a high cut filter to model zero distance "kappa" effects; this is the common observed rapid spectral decay at high frequencies [22]. The quality factor, $Q(f)$, is inversely related to anelastic attenuation. The term $1/R$ shows the geometrical spreading, appropriate for body wave spreading in a whole space. $1/R$ can be changed, once needed, in order to take into account the presence of the postcritical reflections from the Moho discontinuity. $D(f)$ is the site amplification term, which is a function of soil type and frequency.

In extending point source modeling to finite fault modeling, a large fault is divided into N subfaults and each subfault is considered as a small point source, introduced by Hartzell [23]. The rupture spreads radially from the hypocenter. The ground motions of subfaults (each of which is calculated by the stochastic point source method) are summed by a proper delay time in the time domain to obtain the ground motion acceleration. This delay time is related to the distance between each subfault and the observation point. Delay time depends on the location of the hypocenter and the rupture velocity too. Finite fault modeling emphasizes the effects of fault dimension, rupture propagation, directivity and source receiver geometry.

Different methods for the simulation of strong ground motion are available in the literature and selection of the methods depends on the input parameters. It is generally accepted that we should go towards the realistic strong ground motion simulation, as it is applied, for example, for Tehran by Hamzehloo et al. [24]. They used a hybrid method of modal summation and finite difference. This method needs a Q-velocity model and the geometry of the local site condition which is not available for Tabriz city. Furthermore, as there is no record of small events at Tabriz stations, the Empirical Green Function method cannot be applied. Therefore, the stochastic finite fault modeling should be used. This method which needs limited input parameters can be easily applied.

In this study, a program named EXSIM is used for earthquake simulation. EXSIM is a program developed by Motazedian and Atkinson in 2005 for earthquake simulation, based on a dynamic corner frequency using stochastic finite fault modeling [25]. The term EXSIM comes from EXtended fault SIMulation. EXSIM is the new version of FINSIM (FINite fault SIMulation program), which was developed by Beresnev and Atkinson in 1998 [26]. Simulations based on EXSIM produce more realistic time series than those based on FINSIM. In FINSIM, the large subfault size that is required to model very large earthquakes (e.g., $M8$) often produces artificial gaps in the simulated acceleration time series. In EXSIM, a small subfault size is chosen to eliminate any such artifacts in the time series. Characteristics of near fault strong ground motions can induce a pulse in a simulated acceleration time series.

Mavroeidis and Papageorgiou [27] have introduced a novel analytical model that can be used

to include impulsive behavior in the stochastic and other modeling techniques. They showed that the key parameters that define the waveform characteristics of near fault velocity pulses are pulse duration (or period), pulse amplitude and the number and phase of half cycles. They defined an analytical model that describes the near fault velocity pulse in terms of these four parameters determined by empirical data.

Motazedian and Atkinson [25] included a combination of the above analytical and stochastic methods in EXSIM to provide a tool for describing the impulsive behavior of near fault velocity pulses and their influences on the long period ground motions that are observed in many earthquakes. Thus, EXSIM can include a stochastic approach and a combination of analytical and stochastic approaches in finite fault modeling.

For specific near fault records, a combination of the analytical and stochastic approach works well in producing realistic broadband time histories that match both low and high frequency motions. Motazedian and Moinfar [28] used this analytical option of EXSIM in a successful simulation of near field records in the Bam earthquake. In spite of all foregoing strong points for EXSIM, this simulation program has some deficiencies. For example, this program models the earth as a half space, which is not true; considering the earth of two or three layers would give more realistic results. Moreover, soil nonlinearity cannot be noted by EXSIM and, finally, this program has a slight subfault size dependency in the near field, which should be corrected in the future.

Model Parameters

EXSIM requires region specific attenuation and some generic site parameters presented in Table 2. Wells and Coopersmith equations were adopted for calculating the fault dimensions for a moment magnitude of 6.8 (return period of 475 years) [29]. In this research, a California based generic crustal amplification for rock and soil sites, proposed by Boore and Joyner [30], was applied for the stations. Based on present information about the soil type at the stations, a simulation is performed for generic rock sites that are equivalent to NEHRP C [31]. A random slip distribution and location for the hypocenter is assumed because of having no detailed information about the probable asperities in the north Tabriz fault. In this study, the Saragoni-Hart function is used as a window function. In the near source, where there is a subfault size dependency, the Bresnev and Atkinson equation ($\log dl = -2.0 + 0.4M$) is used to calculate the size of the subfaults [32]. Here, EXSIM has been used once without considering its analytical option and the simulations are done once using this option of EXSIM.

Table 2. Model parameters used in stochastic finite fault simulation.

Dip	80
Strike	125
Fault Length (M 6.8)	44 km
Fault Width (M 6.8)	12 km
Fault Length (M 7.0)	59 km
Fault Width (M 7.0)	14 km
Geometrical Spreading	r^{-1}
Ground Motion Duration	$T(R) = T_0 + 0.1R$ $T_0 = 1/(2fa)$ $\log(fa) = 2.41 - 0.533M$
Quality Factor	$147f^{0.97}$
Kappa	0.035
Shear Wave Velocity (β)	3.2 km/s
Rupture Velocity	0.8 β
Density	2.8 g/cm^3
Stress Parameter (475 yr)	20, 40, 60 bars
Pulsing Area Percentage	100%

RESULTS

Results Based on Deaggregation

Seismic hazard deaggregation has been calculated for 2% and 10% probabilities of exceedance over 50 years in Tabriz for Peak Ground Acceleration (PGA) and spectral response acceleration (SA) for the desired periods of 0.1, 0.2, 0.3, 0.5, 1.0 and 2.0 sec. Deaggregation plots for PGA are shown in Figures 2 and 3 for return periods of 475 and 2475 years, respectively. Uniform hazard spectra for these two return periods are calculated for the selected points in Tabriz. An example of uniform hazard spectra and the location of Tabriz stations are shown in Figures 4 and 5, respectively.

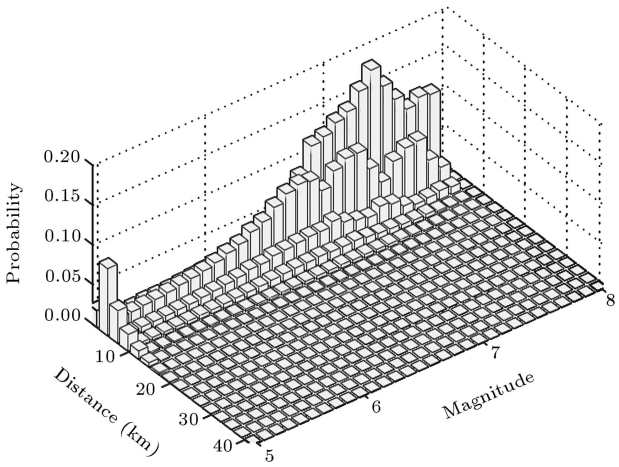

Figure 2. Tabriz deaggregation plot for PGA of 10% exceedance probability in 50 years.

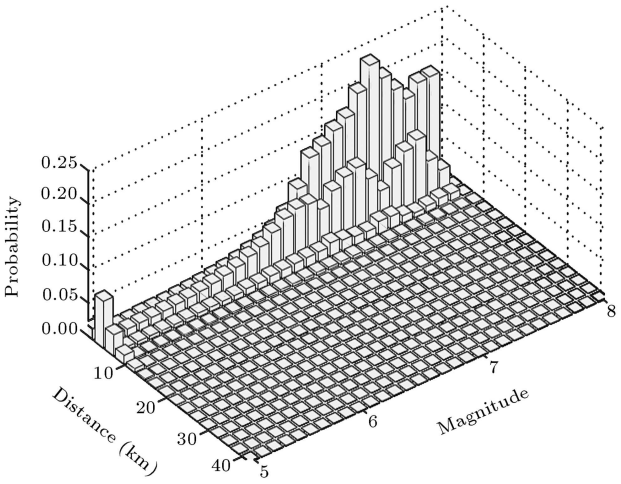

Figure 3. Tabriz deaggregation plot for PGA of 2% exceedance probability in 50 years.

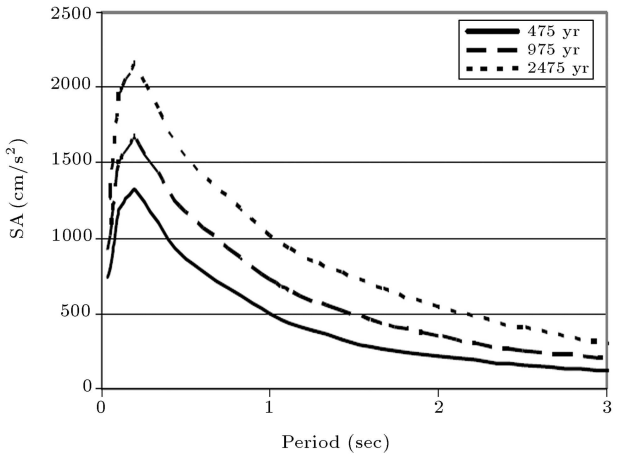

Figure 4. Uniform hazard spectra for return periods of 475, 975 and 2475 years for Tabriz.

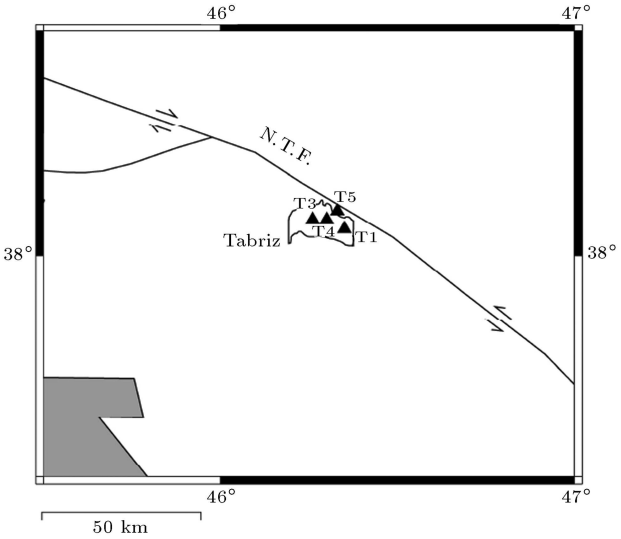

Figure 5. Locations of stations around the North Tabriz Fault.

The mean magnitudes and distances are calculated for PGA and different spectral accelerations, showing for PGA, 6.8 and 3.9 km for a return period of 475 years and 7.0 and 3.3 km for 2475 years, respectively. We have also applied the Kijko and Sellevoll method to estimate the earthquake magnitude [33]. This method, which allows the combination of catalog parts of different qualities is based on a maximum likelihood estimation of earthquake hazard parameters [33,34]. The estimated magnitude is 6.8 for a return period of 475 years, which corresponds to the estimated magnitude based on the deaggregation analysis. The estimated magnitude for a return period of 475 years, based on the Kijko and Sellevoll method, is used for simulation of a strong ground motion due to the activation of the north Tabriz fault.

Results Based on Simulation

Strong ground motions have been simulated at the selected observation points (Figure 5), using the modeling parameters given in Table 2. To simulate strong ground motions generated by the north Tabriz fault, the most dominant source, the method presented by Motazedian and Atkinson [25] has been used, applying the EXSIM program. In this regard, the NEHRP C class has been assumed, based on the soil type information at T1, T3, T4 and T5 stations.

The average shear wave velocities at all stations are in the range of 360 m/s-760 m/s (NEHRP C class). Wells and Coppersmith equations [29] have been used for the estimation of fault dimensions. In this study, stress parameters, $\Delta\sigma_1$, $\Delta\sigma_2$ and $\Delta\sigma_3$, of 20, 40 and 60 bars, respectively, have been considered for a return period of 475 years. It is clear that all stations are very near to the north Tabriz fault and they will experience a high level of ground motion due to the activation of this fault. Figure 6 shows an example of simulated

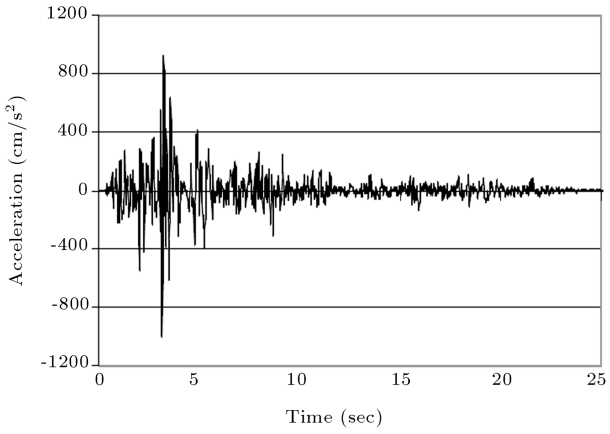

Figure 6. A sample for simulated acceleration time histories at Tabriz 3 station for a 475-year return period and stress parameter of 60 bars.

records at the T3 station. The stress parameter is considered as 60 bars for this simulated record.

The calculated uniform hazard spectrum for a 475-year return period is compared with simulated spectral accelerations, using the above mentioned stress parameters at all stations (Figure 7). Regarding Figure 7, it can be concluded that for the return period of 475 years a stress parameter of about 60 bars generates more compatible spectral accelerations with the corresponding uniform hazard spectrum. Using the stress parameter of 60 bars leads to relatively over-estimated results, reliable enough for seismic design or dynamic analysis. It seems that the stochastic finite fault modeling is more capable of simulating high frequencies rather than low frequencies, because the stochastic finite fault modeling is fundamentally based on the simulation of high frequencies. Moreover, at small distances, near field effects (e.g. directivity) increase the amplitudes of long period pulses.

DISCUSSION

The studies concerned with evaluating seismic hazards require prediction of strong ground motions from earthquakes that pose a potential threat to mankind. Tabriz is classified as a very high hazard region in the NW of Iran according to the GSHAP map [35] and the Iranian code of practice for the seismic resistant design of buildings [36]. Modeling methods can be used to estimate strong ground motions in a hypothetical earthquake for Tabriz, where there is no strong motion data. In this study, a seismic hazard deaggregation and maximum likelihood method are applied to estimate the magnitude for the simulation of strong ground motions for a return period of 475 years. The NTF is considered as the only source in this region based on available historical data.

Mean magnitudes and distances are calculated in the return periods of 475 and 2475 years, for PGA and spectral response accelerations (SA) of 0.1, 0.2, 0.3, 0.5, 1.0 and 2.0 sec. It is observed that the mean magnitude increases as the response period increases.

Reduction in the mean magnitude and distance with a decreasing response period is typical behavior in deaggregation plots [3]. This phenomenon is also observed in Tabriz (Table 3). For a constant return period, mean magnitude increases as the response period increases as shown in Table 3. It can be concluded

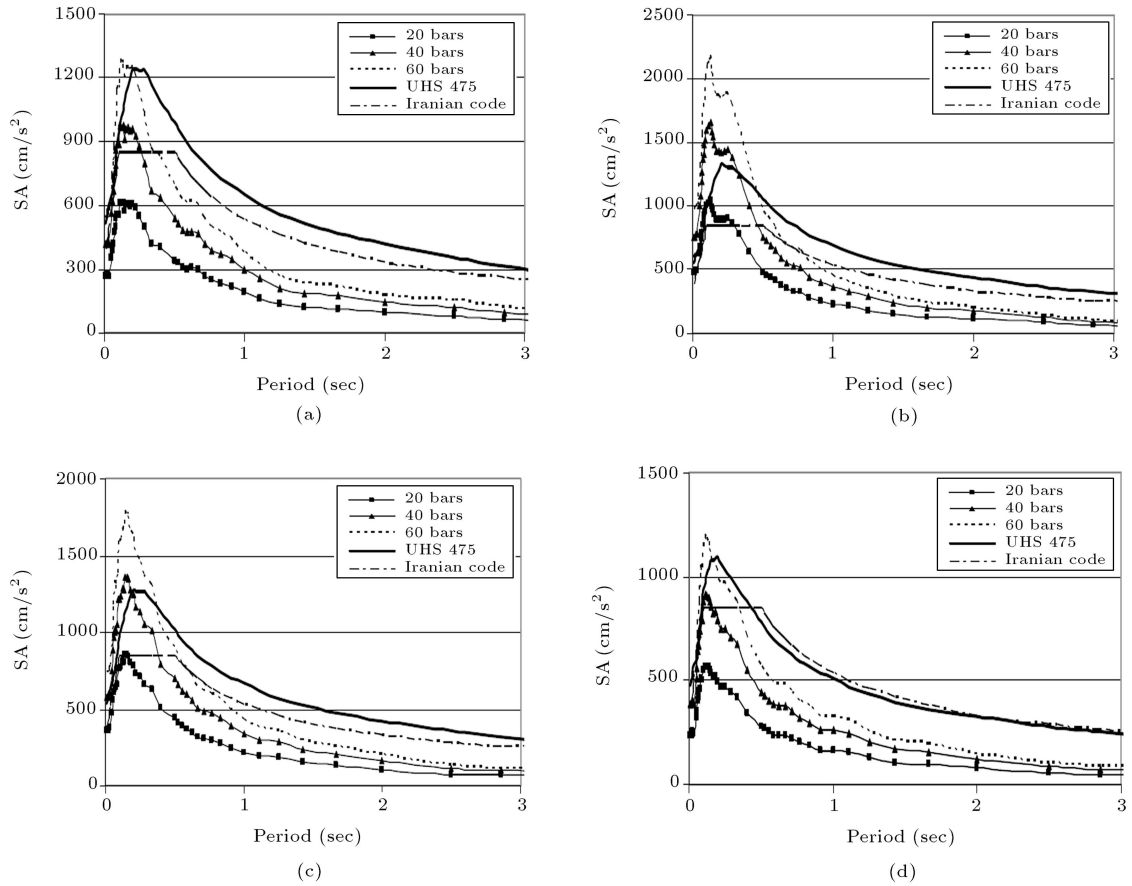

Figure 7. Comparison between uniform hazard spectrum and simulated spectral accelerations at a) Tabriz 1; b) Tabriz 3; c) Tabriz 4; and d) Tabriz 5 stations for a 475-year return period.

Table 3. Mean magnitude and mean distance for different periods in Tabriz.

Return Period	M & R	Spectral Response Period					
		0.1	0.2	0.3	0.5	1.0	2.0
475 yr	Mean magnitude	6.9	7.1	7.2	7.3	7.4	7.5
	Mean distance	4.05	4.16	4.14	4.34	4.39	4.27
2475 yr	Mean magnitude	7.1	7.2	7.3	7.5	7.6	7.7
	Mean distance	3.42	3.47	3.42	3.43	3.38	3.22

that for a constant response period, if the return period increases, the mean magnitude also increases, while the mean distance decreases. In other words, the lower the probability of exceedance, the closer the dominant source to the site, as being reported by Harmsen and Frankel [4] as well.

Strong ground motions have been simulated for a hypothetical earthquake based on the estimated mean magnitude. The magnitude and other required modeling parameters for simulation are presented in Table 2. The seismic hazard deaggregation shows that the north Tabriz fault is the most potential seismic source in the vicinity of Tabriz.

Strong ground motions have been simulated for a return period of 475 years, based on the estimated mean magnitude at T1, T3, T4 and T5 stations in Tabriz. In this study, the EXSIM program has been used to simulate the high frequencies upon the stochastic finite fault modeling. Using these simulated accelerations, the response spectra are calculated and compared with the uniform hazard spectrum at the stations (Figure 7). In this research, the random location of the hypocenter and a random case for slip distribution on the causative fault have been studied. The ground motions, at a particular point, are affected by source, path and site conditions. To consider the source effect on the simulated ground motion, the strike and dip of the north Tabriz fault have been used, based on the available geological information. The effect of the path is considered based on geometrical and anelastic attenuation (Table 2). The frequency dependent equation for Q (quality factor) is used, as $Q(f) = 147f^{0.97}$ [37], and the site condition is considered according to the information given by the Building and Housing Research Center [31].

The seismic moment is considered according to the estimated magnitude, based on the deaggregation analysis and maximum likelihood method. Different stress parameters for the simulation of strong ground motions have been studied in this research because of having no information on stress parameters in this region. In order to take the stress parameter uncertainty into account, stress parameters of 20, 40 and 60 bars have been considered for a return period of 475 years in the simulations. The estimated peak ground accelerations are presented in Table 4 for stress parameters of 20, 40 and 60 bars for a return period of 475 years. Such estimations can be effective in deciding the earthquake resistant design criteria for structures being planned in an area.

The effect of a near source on the simulated ground motions is also considered in EXSIM, based on the mathematical representation of a near fault given by Mavroeidis and Papagerrgiou [27]. The fault rupture dimensions are considered, according to Wells and Coppersmith [29] equations.

In this study, the simulated spectral accelerations, the uniform hazard spectrum and the Iranian code spectrum [36] are compared (Figure 7). It is observed that the Iranian code predicts larger values for periods greater than 1 sec (compared to simulated response spectra) for stress parameters of 20, 40 and 60 bars at all four stations and for a return period of 475 years. This phenomenon is generally observed for strong

Table 4. Simulated PGA using different stress parameters for a return period of 475 year.

Return Period	Station	Longitude	Latitude	Distance (km)	PGA(cm/s^2)		
					$\Delta\sigma_1$	$\Delta\sigma_2$	$\Delta\sigma_3$
475 yr	Tabriz 1	46.35 E	38.06 N	2.36	266	422	553
	Tabriz 3	46.26 E	38.08 N	1.18	475	758	995
	Tabriz 4	46.30 E	38.08 N	1.81	362	575	754
	Tabriz 5	46.33 E	38.10 N	4.90	242	384	503

ground motions recorded in Iran, while the uniform hazard spectrum predicts larger values in comparison with the Iranian code.

The simulated response spectra show higher values at high frequencies, contrasting with the uniform hazard spectrum (Figure 7). This phenomenon is expected because the uniform hazard spectrum is calculated by the seismic hazard analysis, while simulated response spectra are obtained by the records simulated by stochastic modeling. EXSIM can consider the effect of low frequencies in the simulation, which is necessary in the near field simulation. The directivity effect is considered by the mathematical representation of a near fault given by Mavroeidis and Papagerrgiou [27]. The simulated response spectra, which consider the directivity effects given by Mavroeidis and Papagerrgiou, the uniform hazard spectrum and the Iranian code spectrum have been compared in Figure 8. The simulated response spectra are shown for a stress parameter of 60 bars at all four stations (Figure 8). Here, it is observed that the fit between simulated spectra and their corresponding uniform hazard spectrum has been improved by including the directivity effect, especially at high periods, in contrast to Figure 7. The mathematical representation of near field ground motions given by Mavroeidis and Papagerrgiou [27] has no influence on PGA and only changes the low frequency content in the simulated records.

As soil nonlinearity cannot be noted by stochastic finite fault simulation, the change in the frequency content with time and the nonlinear soil amplification of ground motions are not modeled in this study.

CONCLUSION

In this research, the most potential source for Tabriz is identified upon the seismic hazard deaggregation and the mean magnitudes and distances are estimated for return periods of 475 and 2475 years. For a return period of 475 years, the seismic hazard deaggregation and maximum likelihood method, proposed by Kijko and Sellevoll [33], lead to a magnitude of 6.8, used in

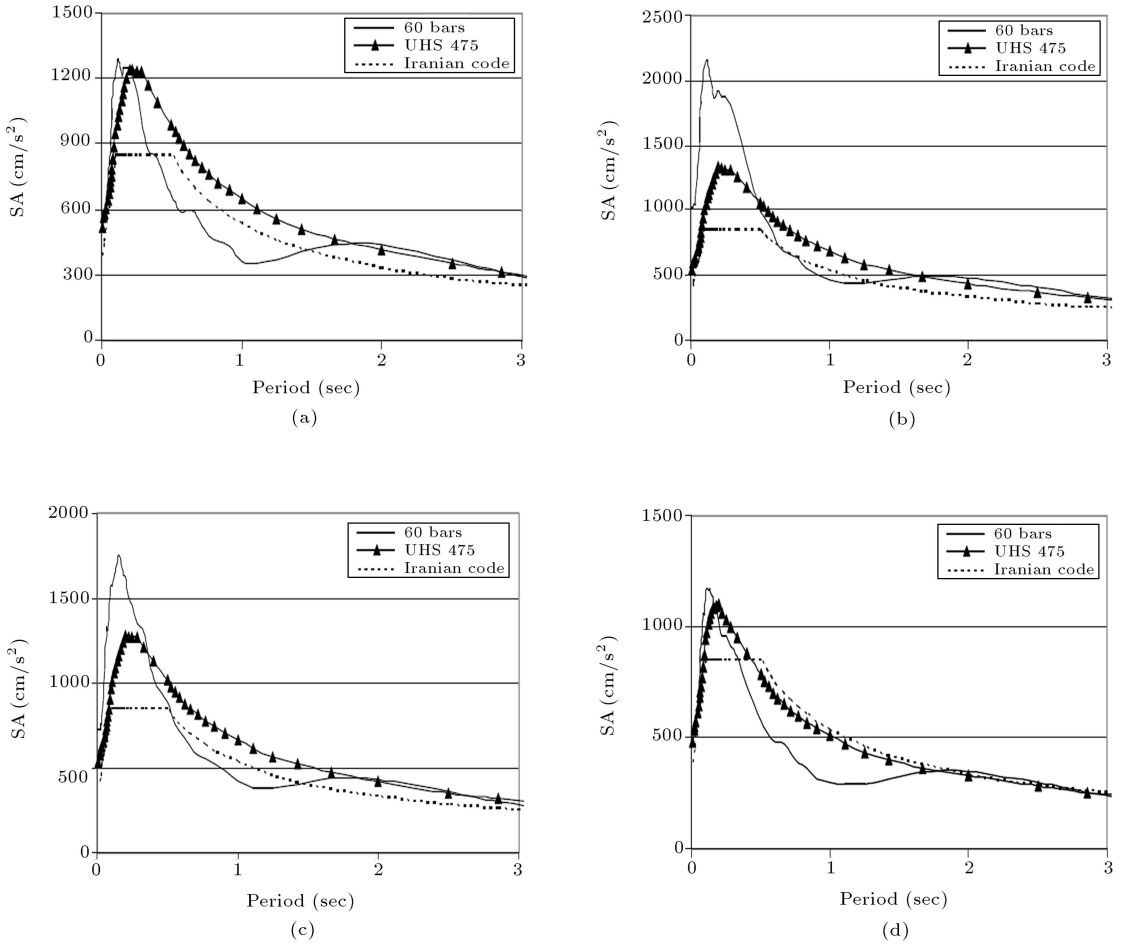

Figure 8. Comparison between uniform hazard spectrum and simulated spectral acceleration ($\Delta\sigma = 60$ bar) at a) Tabriz 1; b) Tabriz 3; c) Tabriz 4; and d) Tabriz 5 stations for a 475-year return period using deterministic option of EXSIM.

the earthquake simulation, upon stochastic finite fault modeling. Using this modeling, strong ground motions are simulated for a return period of 475 years at 4 stations in Tabriz. Comparing the simulated spectral accelerations and their corresponding uniform hazard spectra, it is concluded that more compatible spectral accelerations with the corresponding uniform hazard spectra are generated by a stress parameter of about 60 bars for a return period of 475 years.

ACKNOWLEDGMENTS

The authors wish to express their gratefullness to the Department of Civil Engineering at Sharif University of Technology for supporting this research. The constructive comments from anonymous reviewers on this manuscript are also greatly appreciated.

REFERENCES

1. Sokolov, V.Y. "Hazard-consistent ground motions: Generation on the basis of uniform hazard Fourier spectra", *Bull. Seism. Soc. Am.*, **90**, pp. 1010-1027 (2000).
2. Bazzurro, P. and Cornell, C.A. "Disaggregation of seismic hazard", *Bull. Seism. Soc. Am.*, **89**, pp. 501-520 (1999).
3. Harmsen, S., Perkins, D. and Frankel, A. "Deaggregation of probabilistic ground motions in the central and eastern United States", *Bull. Seism. Soc. Am.*, **89**, pp. 1-13 (1999).
4. Harmsen, S. and Frankel, A. "Geographic deaggregation of seismic hazard in the United States", *Bull. Seism. Soc. Am.*, **91**, pp. 13-26 (2001).
5. Hessami, K., Pantosti, D., Tabassi, H., Shabanian, E., Abbassi, M.R., Feghhi, K. and Solaymani, S. "Paleoearthquakes and slip rates of the north Tabriz fault, NW Iran: preliminary results", *Annals of Geophysics*, **46**, pp. 903-915 (2003).
6. Berberian, M. and Arshadi, S. "On the evidence of the youngest activity of the north Tabriz fault and the seismicity of Tabriz city", *Geol. Surv. Iran Rep.*, **39**, pp. 397-418 (1976).
7. Karakhanian, A.S., Trifonov, V.G., Philip, H., Avagyan, A., Hessami, H., Jamali, F., Bayraktutan, M.S., Bagdassarian, H., Arakelian, S., Davtian, V. and Adilkhanyan, A. "Active faulting and natural hazards in Armenia, eastern Turkey and northwestern Iran", *Tectonophysics*, **380**(3-4), pp. 189-219 (2004).
8. Berberian, M. and Yeats, R.S. "Patterns of historical earthquake rupture in the Iranian plateau", *Bull. Seism. Soc. Am.*, **89**, pp. 120-139 (1999).
9. Masson, F., Djamour, Y., Van Gorp, S., Chery, J., Tatar, M., Tavakoli, F., Nankali, H. and Vernant, P. "Extension in NW Iran driven by the motion of the South Caspian Basin", *Earth and Planetary Science Letters*, **252**, pp. 180-188 (2006).
10. Frankel, A. "Mapping seismic hazard in the central and eastern United States", *Seism. Res. Lett.*, **66**(4), pp. 8-21 (1995).
11. Frankel, A., Mueller, C., Barnlaard, T., Perkins, D., Leyendecker, E., Dickman, N., Hanson, S. and Hopper, M. "National seismic-hazard maps: Documentation", *U.S. Geol. Surv. Open-File Rept. 96-532*, p. 110 (1996).
12. Bernreuter, D.L., *Determining the Controlling Earthquake from Probabilistic Hazards for the Proposed Appendix B*, Lawrence Livermore National Laboratory UCRL-JC-111964 (1992).
13. Cramer, C.H. and Petersen, M.D. "Predominant seismic source distance and magnitude maps for Los Angeles, Orange and Ventura counties, California", *Bull Seism. Soc. Am.*, **86**, pp. 1645-1649 (1996).
14. McGuire, R.K. and Shedloek, K.M. "Statistical uncertainties in seismic hazard evaluations in the United States", *Bull. Seism. Soc. Am.*, **71**, pp. 1287-1308 (1981).
15. Sadigh, K., Chang, C.Y., Egan, J.A., Makdisi, F. and Youngs, R.R. "Attenuation relationships for shallow crustal earthquakes based on California strong motion data", *Seism. Res. Lett.*, **68**, pp. 180-189 (1997).
16. Atkinson, G. and Silva, W. "Stochastic modeling of California ground motions", *Bull. Seism. Soc. Am.*, **90**, pp. 255-274 (2000).
17. Campbell, K.W. and Bozorgnia, Y. "Updated near-source ground motion attenuation relations for the horizontal and vertical components of peak ground acceleration and acceleration response spectra", *Bull. Seism. Soc. Am.*, **93**, pp. 314-331 (2003).
18. Boore, D. "Stochastic simulation of high-frequency ground motions based on seismological models of the radiated spectra", *Bull. Seism. Soc. Am.*, **73**, pp. 1865-1894 (1983).
19. Aki, K. "Scaling law of seismic spectrum", *J. Geophys. Res.*, **72**, pp. 1217-1231 (1967).
20. Brune, J. "Tectonic stress and the spectra of seismic shear waves from earthquakes", *J. Geophys. Res.*, **75**, pp. 4997-5009 (1970).
21. Brune, J. "Correction", *J. Geophys. Res.*, **76**, p. 5002 (1971).
22. Anderson, J. and Hough, S. "A model for the shape of the Fourier amplitude spectrum of acceleration at high frequencies", *Bull. Seism. Soc. Am.*, **74**, pp. 1969-1993 (1984).
23. Hartzell, S. "Earthquake aftershocks as Green's functions", *Geophys. Res. Letters*, **5**, pp. 1-14 (1978).
24. Hamzehloo, H., Vaccari, F. and Panza, G.F. "Towards a reliable seismic microzonation in Tehran, Iran", *Engineering Geology*, **93**, pp. 1-16 (2007).
25. Motazedian, D. and Atkinson, G. "Stochastic finite fault modeling based on a dynamic corner frequency", *Bull. Seism. Soc. Am.*, **95**, pp. 995-1010 (2005).

26. Beresnev, I. and Atkinson, G. "FINSIM - a FORTRAN program for simulating stochastic acceleration time histories from finite faults", *Seism. Res. Lett.*, **69**, pp. 27-32 (1998).

27. Mavroeidis, G.P. and Papageorgiou, A.S. "A mathematical representation of near-fault ground motions", *Bull. Seism. Soc. Am.*, **93**, pp. 1099-1131 (2003).

28. Motazedian, D. and Moinfar, A.A. "Hybrid stochastic finite fault modeling of 2003, M6.5, Bam Earthquake (Iran)", *J. Seism.*, **10**, pp. 91-103 (2006).

29. Wells, D. and Coppersmith, K. "New empirical relationships among magnitude, rupture length, rupture width, rupture area and surface displacement", *Bull. Seism. Soc. Am.*, **84**, pp. 974-1002 (1994).

30. Boore, D. and Joyner, W. "Site amplifications for generic rock sites", *Bull. Seism. Soc. Am.*, **87**, pp. 327-341 (1997).

31. Haeri, M., *Seismic Microzonation and Design Spectrum for Metropolitan Area- Tabriz City*, The Interior Ministry, National Disaster Task Force, Earthquake and Land Slide Hazards Committee, Published by Building and Housing Research Center, Iran (2005).

32. Beresnev, I. and Atkinson, G. "Subevent structure of large earthquakes - A ground motion perspective", *Geophiys. Res. Lett.*, **28**, pp. 53-56 (2001).

33. Kijko, A. and Sellevoll, M.A. "Estimation of earthquake hazard parameters from incomplete data files. Part I. Utilization of extreme and complete catalogs with different threshold magnitudes", *Bull. Seism. Soc. Am.*, **79**, pp. 645-654 (1989).

34. Kijko, A. and Sellevoll, M.A. "Estimation of earthquake hazard parameters from incomplete data files. Part II. Incorporation of magnitude heterogeneity", *Bull. Seism. Soc. Am.*, **82**, pp. 120-134 (1992).

35. Tavakoli, B. and Ghafory-Ashtiany, M. "Seismic hazard assessment of Iran", *Annali di Geofisica*, **42**(6), pp. 1013-1021 (1999).

36. *Iranian Building Code, Standard 2800*, 3rd Ed., Published by Building and Housing Research Center, Iran (2006).

37. Farahbod, A.M. and Alahyarkhani, M. "Attenuation and propagation of seismic waves in Iran", *Fourth International Conference of Earthquake Engineering and Seismology*, Tehran, Iran (2003).